Progress In Electromagnetics Research, PIER 80, 349–368, 2008

MUTUAL EXTERNAL INDUCTANCE IN STRIPLINE STRUCTURES

M. Y. Koledintseva, J. L. Drewniak, T. P. Van Doren
D. J. Pommerenke and M. Cocchini

Electromagnetic Compatibility Laboratory
University of Missouri-Rolla
1870 Miner Circle, Rolla, MO 65409-0040, USA

D. M. Hockanson

Sun Microsystems, Inc.
901 San Antonio Road, Palo Alto, CA 94303, USA

Abstract—The Method of Edge Currents (MEC) proposed in our previous paper [1] is applied herein for calculating the mutual external inductance associated with fringing magnetic fields that wrap ground planes of a stripline structure. This method employs a quasi-static approach, image theory, and direct magnetic field integration. The resultant mutual external inductance is frequency-independent. The approach has been applied to estimating mutual inductance for both symmetrical and asymmetrical stripline structures. Offset of the signal trace from the centered position both in horizontal and vertical directions is taken into account in asymmetrical structures. The results are compared with numerical simulations using the CST Microwave Studio Software.

1. INTRODUCTION

The *Method of Edge Currents (MEC)* was proposed in our previous paper [1]. This method employs a quasi-static (quasi-magnetostatic) approach, image theory, and direct magnetic field integration for calculating the *mutual external inductance* of a planar transmission line structure with ground planes of finite width. This inductance is of interest from electromagnetic immunity point of view, since it is a culprit of "*ground plane noise*", or a *common-mode voltage*, that appears on the reference plane due to fringing magnetic fields wrapping

the plane, and drives unintentional "antennas" formed by parts of the electronic equipment [2–8]. This mutual external inductance associated with fringing magnetic fields wrapping the ground plane of a stripline structure is defined as the mutual inductance between the signal current loop and the common mode "antenna" current loop located either above the top ground plane, or beneath the bottom ground plane. In [1], it was shown that when an infinitely wide ground plane is cut to a finite width, the residual surface current on the "tails" that are cut off may be redistributed on the edges of the ground plane of finite width, forming edge currents. The mutual external inductance of interest is determined by the magnetic fluxes produced by these edge currents. At the same time, the contributions to the magnetic flux by the currents from the signal trace and finite-size ground plane (or planes) completely compensate each other. The method of edge currents was applied and tested to estimating mutual inductance for symmetrical and asymmetrical microstrip lines [1]. Along with microstrip structures [9–14], there is an increasing interest to the analysis of stripline geometries, because of their applications for antenna and interconnect design [15–20]. In the present paper, the method of edge currents is extended for symmetrical and asymmetrical stripline structures. So far, there are no publications on calculating this kind of mutual inductance for stripline geometries. However, recently a paper utilizing image theory together with a suitable quasi-static Green's function approach was published, and it contains analytical closed-form expressions for currents on the ground planes of stripline structures [21].

Mutual external inductance associated with fringing magnetic fields in a stripline structure with a ground plane of finite size is considered herein using the assumptions similar to those applied to the microstrip case in [1], so that the quasi-magnetostatic approach and image theory are applicable. The resultant per-unit-length inductance can be calculated, and it will be independent of frequency (though in the general case, when considering higher frequencies and radiation from the structure, it will be frequency-dependent).

A stripline, as compared to a microstrip structure, is almost completely shielded, and the electromagnetic field is much better contained in the stripline structure than in the microstrip. There is almost no field at the edges of the stripline, if the width of the ground planes is $w_g \geq w_s + \alpha(h_1 + h_2)$, where h_1 and h_2 are the distances from the trace to the bottom and top ground planes, respectively, w_s is the width of the trace, and the coefficient $2 \leq \alpha \leq 3$ [22]. However, when the width of the ground plane is small (e.g., $w_g/h < 7$ in a symmetrical stripline with $h = h_1 = h_2$), then the fringing fields are of importance.

A quasistatic approach for a stripline is valid, if only the TEM mode propagates in the line. This happens, if the cross-sectional sizes are much smaller than the wavelength in the transmission line. The higher-order modes in a stripline do not propagate, if the equivalent width of a signal strip is smaller than half of the wavelength in the dielectric of the stripline ($w_{s\,eqv} < \lambda_{diel}/2$), and also if the distance between the ground planes is $h_1 + h_2 < \lambda_{diel}/2$. If these two conditions are satisfied at the maximum operating frequency, then this is a single-mode transmission line. The equivalent width of the strip $w_{s\,eqv} = w_s + \Delta w_s$ is greater than the geometrical width w_s due to the edge effect. The increment of the strip width can be calculated approximately as [22]

$$\Delta w_s = \frac{2(h_1+h_2)}{\pi}\left[\ln\left(2+\frac{t}{h_1+h_2}\right)+\frac{t}{2(h_1+h_2)}\ln\left(\frac{2(h_1+h_2)}{t}+1\right)\right], \tag{1}$$

where t is the thickness of the signal trace. For very thin traces ($t \ll h_1 + h_2$), the effective increment of the width of the trace is $\Delta w_s \approx 0.45(h_1 + h_2) + 1.1 \cdot t$ [22].

2. MODEL OF MUTUAL EXTERNAL INDUCTANCE

2.1. Symmetrical Stripline Geometry

The edge currents in the stripline case are found analogous to the microstrip case, but since there are now two ground planes, there are multiple image sources at $z = (2n-1)h,\ n \in \Im$ (integer), as shown in Figure 1.

First assume that the signal trace is a thin filament, and, correspondingly, all of the image sources are thin filaments, too. Later we will consider the case of a signal trace of finite width as well. Because of the images from the infinite ground planes, the currents have alternating signs, as is shown in Figure 1. The static magnetic field produced by any source placed at $z = (2n-1)h$ has the following y-component at any point along the plane $(y, 0)$,

$$H^{+}_{y(2n-1)h} = \frac{(-1)^{n+1} \cdot I_S \cdot (2n-1)h}{2\pi\left((2n-1)^2h^2 + y^2\right)}. \tag{2}$$

Fields from symmetrical sources are doubled, so the total y-component of the magnetic field at the point $(y, 0)$ is

$$H_y = \frac{I_S}{\pi} \cdot \sum_{n=1}^{\infty} \frac{(-1)^{n+1} \cdot (2n-1)h}{(2n-1)^2h^2 + y^2}. \tag{3}$$

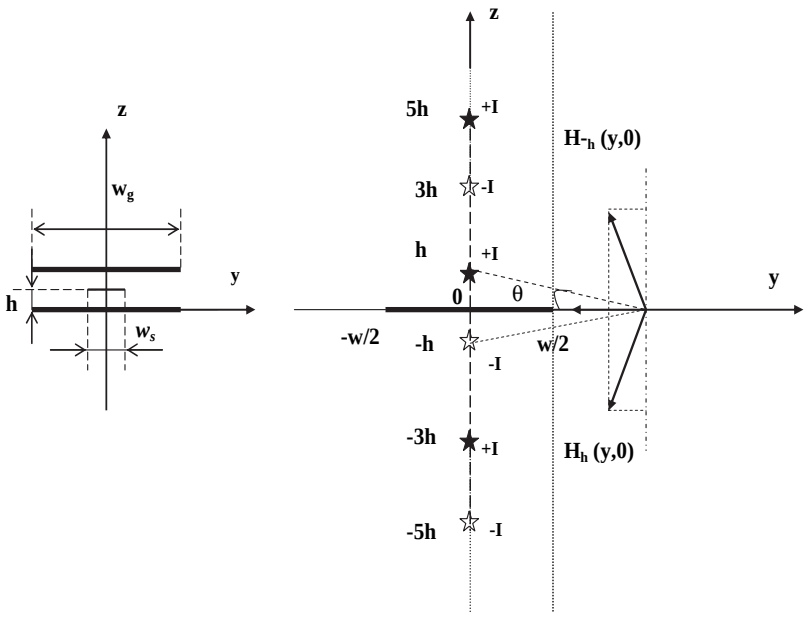

Figure 1. Stripline cross-section geometry and static image theory application.

The edge current source to be placed at the point $y = w_g/2$ is then found from

$$\Delta I_1 = \int\limits_{w_g/2}^{+\infty} H_y dy = \frac{I_S}{\pi} \cdot \sum_{n=1}^{+\infty} (-1)^{n+1} \arctan\left(\frac{y}{(2n-1)h}\right)\Bigg|_{w_g/2}^{+\infty}, \quad (4)$$

or

$$\Delta I_1 = \frac{I_S}{\pi} \cdot \sum_{n=1}^{+\infty} (-1)^{n+1} \cdot \lim_{y\to+\infty} \left(\arctan\left(\frac{y}{(2n-1)h}\right) - \arctan\left(\frac{w_g}{2(2n-1)h}\right)\right). \quad (5)$$

It can be shown that the limit in (5) is

$$\lim_{N\to+\infty} \sum_{n=1}^{N} (-1)^{n+1} \lim_{y\to+\infty} \left(\arctan\left(\frac{y}{(2n-1)h}\right) - \arctan\left(\frac{w_g}{2(2n-1)h}\right)\right) = \frac{h}{w_g}. \quad (6)$$

Then, the resultant edge current in a symmetrical stripline case with a filamentary signal trace is

$$\Delta I_{fil} = \Delta I_{1,2,3,4} = \frac{I_S}{\pi} \cdot \left(\frac{h}{w_g} \right). \tag{7}$$

The same result can be obtained from the current balance equation and analogy with the microstrip case. In the stripline, an edge current (7) is half that of the microstrip case (6), and this is intuitively clear because of the symmetry.

Calculation of the edge currents is more complicated, if the signal trace is of finite width w_s. Assume that the current density across the signal trace of the width w_s is distributed evenly, even though this is an approximation [21],

$$J_S = \frac{I_S}{w_s}. \tag{8}$$

According to the image principle, there is a set of distributed currents of alternating signs, and the magnetic field produced by these currents at any point y on the ground planes is

$$H_y = \frac{I_S}{\pi \cdot w_s} \cdot \int\limits_{-w_s/2}^{w_s/2} \sum_{n=1}^{\infty} \frac{(-1)^{n+1} \cdot (2n-1)h}{(2n-1)^2 h^2 + (y-y')^2} dy'. \tag{9}$$

Then, from the boundary conditions on the perfect electric conductors of the ground planes, the induced current density on each ground plane is

$$J_g(y) = \frac{I_S}{\pi \cdot w_s} \cdot \int\limits_{-w_s/2}^{w_s/2} \sum_{n=1}^{\infty} \frac{(-1)^{n+1} \cdot (2n-1)h}{(2n-1)^2 h^2 + (y-y')^2} dy'. \tag{10}$$

The edge currents in the symmetrical stripline are all equal, and they are found by the integration

$$\Delta I = \Delta I_{1,2,3,4} = \int\limits_{w_g/2}^{\infty} J_g(y) dy. \tag{11}$$

The current balance must fulfill

$$I_S = 2I_g + 4\Delta I, \tag{12}$$

where the total current on each ground plane is

$$I_g = \int_{-\infty}^{\infty} J_g(y)dy. \tag{13}$$

Now consider magnetic fluxes. Assume that the structure is translationally invariant along the x-axis, as is shown in Figure 2. The per-unit-length magnetic flux is found by integrating along $z = (-\infty, -R)$, where R is the radius of the rounded edges of the ground

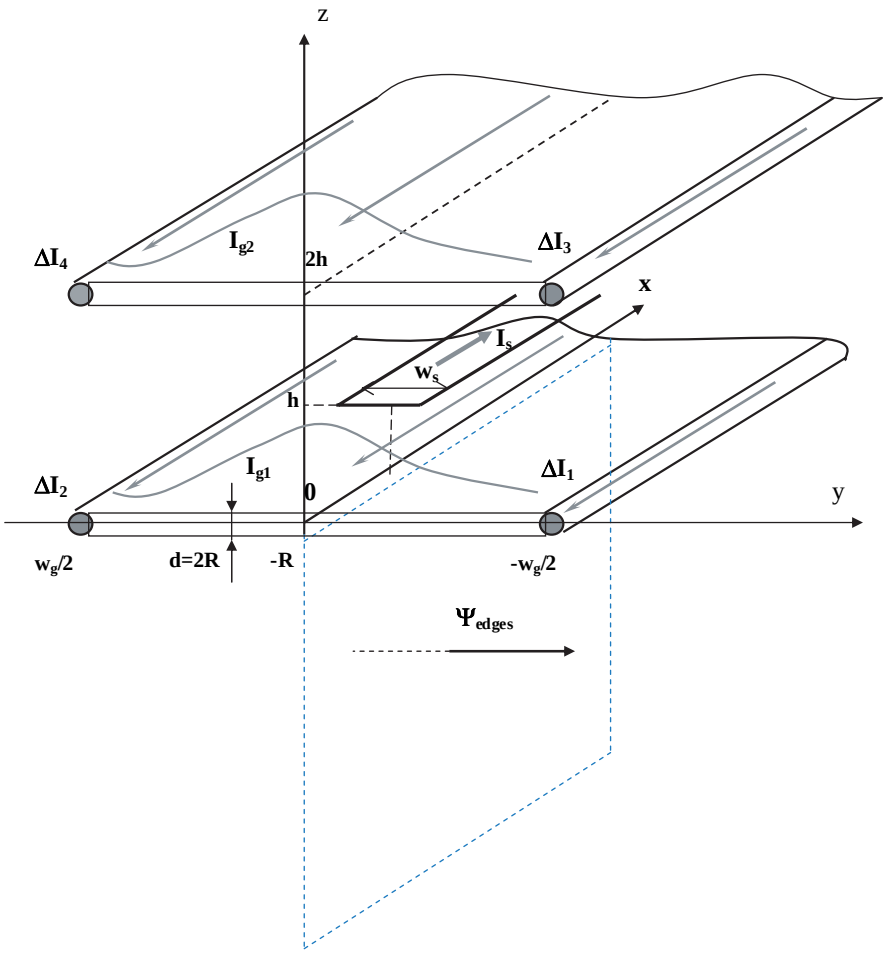

Figure 2. Magnetic flux passing through the contour for calculating of mutual inductance in a symmetrical stripline case.

planes ($d = 2R$ is the thickness of a ground plane). If ground planes of the stripline are infinitely wide, there is no fringing magnetic field, and there is no magnetic flux outside the stripline structure,

$$\Psi_S + \Psi_\infty^{bot} + \Psi_\infty^{top} = 0, \tag{14}$$

where Ψ_∞^{bot} and Ψ_∞^{top} are fluxes produced by infinite bottom and top ground planes, respectively.

At the same time, these fluxes are comprised of fluxes of the finite ground planes and fluxes by the cut-off current "tails",

$$\begin{aligned} \Psi_\infty^{bot} &= \Psi_g^{bot} + \Psi_{tails}^{bot}; \qquad \Psi_\infty^{top} = \Psi_g^{top} + \Psi_{tails}^{top}; \\ \Psi_{tails}^{bot} &= \Psi_{tail1} + \Psi_{tail2}; \quad \Psi_{tails}^{top} = \Psi_{tail3} + \Psi_{tail4}. \end{aligned} \tag{15}$$

On the other hand, if the concept of edge currents is used, the total fringing magnetic field flux above the structure ("up") and below the structure ("down") is

$$\Psi = \Psi_{up} + \Psi_{down} = \Psi_S + \Psi_g^{bot} + \Psi_g^{top} + \Psi_{edges}, \tag{16}$$

where

$$\Psi_{edges} = \sum_{i=1}^{4} \Psi_{edge\ i}, \tag{17}$$

and the notations of the edges are as in Figure 2. In the symmetrical case, all the fluxes by the edge currents are the same. Then, as follows from (14)–(17),

$$\begin{aligned} \Psi_{down} &= \Psi_{edge\,1} - \Psi_{tail\,1} + \Psi_{edge\,2} - \Psi_{tail\,2}; \\ \Psi_{up} &= \Psi_{edge\,3} - \Psi_{tail\,3} + \Psi_{edge\,4} - \Psi_{tail\,4}. \end{aligned} \tag{18}$$

Herein, consider only the mutual external inductance associated with the flux Ψ_{down} under the bottom ground plane. The flux Ψ_{up} is in the upper part of space above the top ground plane, and the corresponding mutual inductance may be considered in the similar way. If the "tail currents" had not been cut off, they would have produced the fluxes

$$\begin{aligned} \Psi_{tail1} = \Psi_{tail2} &= \frac{\mu_0}{2\pi} \int\limits_{w_g/2}^{\infty} J_g(y) \int\limits_{-\infty}^{-R} \frac{R-z}{(R-z)^2+y^2} dz dy; \\ \Psi_{tail3} = \Psi_{tail4} &= \frac{\mu_0}{2\pi} \int\limits_{w_g/2}^{\infty} J_g(y) \int\limits_{-\infty}^{-R} \frac{R+2h-z}{(R+2h-z)^2+y^2} dz dy. \end{aligned} \tag{19}$$

If the edge-current distribution on the rounded edges with radius R is introduced, then the method of calculating fluxes from the edges is the same as described for a microstrip line in [1, see Equations (32)–(37)], with $J_{edge\ i} = \dfrac{\Delta I_i}{\pi R},\ i = 1 \ldots 4.$

$$H^{top}_{y\ edge\ 1,2} = \int\limits_0^{\pi/2} \frac{J_{edge\ 1,2} R \cdot \left(\dfrac{w_g}{2} + R\sin\alpha\right)}{2\pi\left(\left(\dfrac{w_g}{2} + R\sin\alpha\right)^2 + (R\cos\alpha - z)^2\right)} d\alpha;$$
$$H^{bot}_{y\ edge\ 1,2} = \int\limits_0^{\pi/2} \frac{J_{edge\ 1,2} R \cdot \left(\dfrac{w_g}{2} + R\sin\alpha\right)}{2\pi\left(\left(\dfrac{w_g}{2} + R\sin\alpha\right)^2 + (R\cos\alpha + z)^2\right)} d\alpha; \tag{20}$$

and

$$H^{top}_{y\ \text{edge}\ 3,4} = \int\limits_0^{\pi/2} \frac{J_{edge3,4} R \cdot \left(\dfrac{w_g}{2} + R\sin\alpha\right)}{2\pi\left(\left(\dfrac{w_g}{2} + R\sin\alpha\right)^2 + (R\cos\alpha - z + 2h)^2\right)} d\alpha;$$
$$H^{bot}_{y\ edge\ 3,4} = \int\limits_0^{\pi/2} \frac{J_{edge\ 1,2} R \cdot \left(\dfrac{w_g}{2} + R\sin\alpha\right)}{2\pi\left(\left(\dfrac{w_g}{2} + R\sin\alpha\right)^2 + (R\cos\alpha + z + 2h)^2\right)} d\alpha. \tag{21}$$

Then the corresponding edge fluxes are

$$\Psi_{edge\ i} = \mu \cdot \int\limits_{-\infty}^{-R} \left(H^{top}_{y\ edge\ i} + H^{bot}_{y\ edge\ i}\right) dz \quad \text{for} \quad i = 1 \ldots 4. \tag{22}$$

The results of computations of the external mutual inductance in a symmetrical stripline as a function of the ratio w_g/h are presented in Figure 3. The results are obtained using the *method of edge currents*, as well as the *CST Microwave Studio (CST MWS)* software. The agreement is comparatively good for $w_g/h < 10$. Computations show that the "tail" current fluxes are negligible compared to the edge current fluxes, similar to the microstrip case, so only the edge currents may be taken into account.

2.2. Asymmetrical Stripline Geometry

A stripline with both horizontal and vertical offsets of the signal trace from the center is shown in Figure 4. The total y-component of

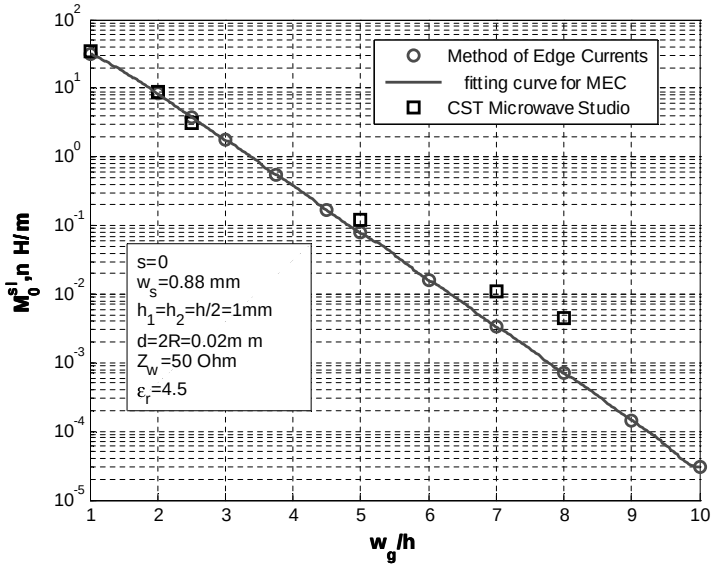

Figure 3. Mutual inductance associated with fringing magnetic fields in a symmetrical stripline geometry as a function of the ratios w_g/h.

magnetic field along the surface of the bottom and top ground planes ($z = 0$ and $z = 2h$) are the same, if the distance from the trace to both ground planes is the same. In the general case, $h_1 \neq h_2$, where h_1 is the distance from the strip to the lower ground plane, h_2 is the distance to the upper ground plane, and $h_1 + h_2 = 2h$.

For the sake of simplicity, assume that there is a filament signal trace with current I_S. Let us first consider the magnetic field on the bottom ground plane. According to the image principle, the currents contributing to the magnetic field on the bottom plane are $-I_S$ at height h_1, $+I_S$ at height $h_1 + 2h_2$, $-I_S$ at height $3h_1 + 2h_2$, $+I_S$ at height $3h_1 + 4h_2$, $-I_S$ at height $5h_1 + 4h_2$, *etc.* Using mathematical induction, the y-component of the total magnetic field on the bottom ground plane is

$$H_{y\Sigma}^{bot} = \frac{I_S}{\pi} \cdot \left(\begin{array}{l} \displaystyle\sum_{n=1}^{\infty} \frac{(-1)^{2n-1} \cdot (2n-1)h_1 + (2n-2)h_2}{((2n-1)h_1 + (2n-2)h_2)^2 + (y-s)^2} + \\ \displaystyle\sum_{n=1}^{\infty} \frac{(-1)^{2n} \cdot (2n-1)h_1 + 2nh_2}{((2n-1)h_1 + 2nh_2)^2 + (y-s)^2} \end{array} \right), \quad (23)$$

where s is a horizontal offset of the signal trace (along y-coordinate). The y-component of the magnetic field on the top ground plane can

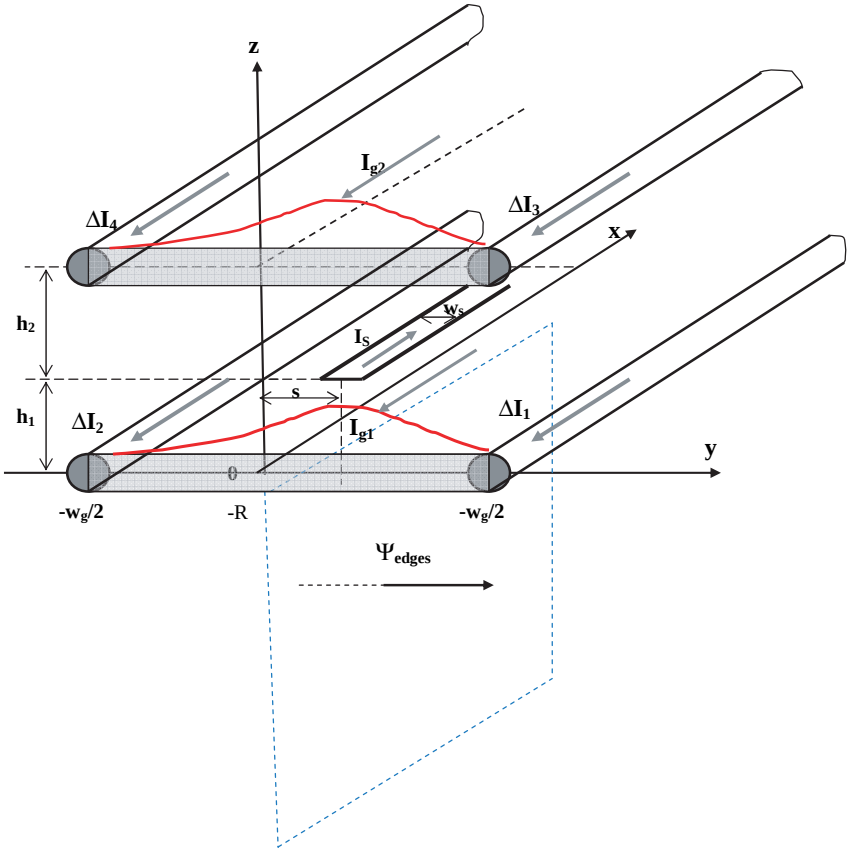

Figure 4. Geometry of the stripline with a shifted strip from the center for fringing magnetic flux calculation.

be derived analogously, though for the top plane, the heights h_1 and h_2 are interchanged as compared to (23). Then,

$$H_{y\Sigma}^{top} = \frac{I_S}{\pi} \cdot \left(\begin{array}{l} \sum\limits_{n=1}^{\infty} \dfrac{(-1)^{2n-1} \cdot (2n-1)h_2 + (2n-2)h_1}{((2n-1)h_2 + (2n-2)h_1)^2 + (y-s)^2} + \\ \sum\limits_{n=1}^{\infty} \dfrac{(-1)^{2n} \cdot (2n-1)h_2 + 2nh_1}{((2n-1)h_2 + 2nh_1)^2 + (y-s)^2} \end{array} \right). \quad (24)$$

Introducing the following notations

$$\begin{aligned} a_n &= (2n-1)h_1 + (2n-2)h_2; \\ b_n &= (2n-1)h_1 + 2nh_2; \\ c_n &= (2n-1)h_2 + (2n-2)h_1; \\ d_n &= (2n-1)h_2 + 2nh_1, \end{aligned} \tag{25}$$

(23) and (24) can be written in a more compact form as

$$\begin{aligned} H_{y\Sigma}^{bot} &= \frac{I_S}{\pi} \cdot \left(\sum_{n=1}^{\infty} \frac{(-1)^{2n-1} \cdot a_n}{a_n^2 + (y-s)^2} + \sum_{n=1}^{\infty} \frac{(-1)^{2n} \cdot b_n}{b_n^2 + (y-s)^2} \right); \\ H_{y\Sigma}^{top} &= \frac{I_S}{\pi} \cdot \left(\sum_{n=1}^{\infty} \frac{(-1)^{2n-1} \cdot c_n}{c_n^2 + (y-s)^2} + \sum_{n=1}^{\infty} \frac{(-1)^{2n} \cdot d_n}{d_n^2 + (y-s)^2} \right). \end{aligned} \tag{26}$$

It should be mentioned that the series in (26) contain alternating-sign terms. Such series are known to be slowly convergent. In practical computations, it might be necessary to take at least 10^8 terms in each series to assure the convergence. However, combining terms in these series as

$$\begin{aligned} H_{y\Sigma}^{bot} &= \frac{I_S}{\pi} \cdot \sum_{n=1}^{\infty} \left(\frac{(-1)^{2n-1} \cdot a_n}{a_n^2 + (y-s)^2} + \frac{(-1)^{2n} \cdot b_n}{b_n^2 + (y-s)^2} \right); \\ H_{y\Sigma}^{tup} &= \frac{I_S}{\pi} \cdot \sum_{n=1}^{\infty} \left(\frac{(-1)^{2n-1} \cdot c_n}{c_n^2 + (y-s)^2} + \frac{(-1)^{2n} \cdot d_n}{d_n^2 + (y-s)^2} \right), \end{aligned} \tag{26a}$$

dramatically improves convergence and speed of computations. Using Maple 10 software, it is possible to get summation up to infinity.

The edge currents on the bottom and on the top planes are

$$\begin{aligned} \Delta I_1(s) &= \int_{w/2}^{\infty} H_{y\Sigma}^{bot} \cdot dy; \quad \Delta I_2(s) = \int_{-\infty}^{-w/2} H_{y\Sigma}^{bot} \cdot dy; \\ \Delta I_3(s) &= \int_{w/2}^{\infty} H_{y\Sigma}^{top} \cdot dy; \quad \Delta I_4(s) = \int_{-\infty}^{-w/2} H_{y\Sigma}^{top} \cdot dy. \end{aligned} \tag{27}$$

Now consider the case when the signal trace is of finite width w_s, and there is a uniform current density across the strip, $J_S = I_S/w_s$.

Then the values of the magnetic field (and the corresponding current densities) on the bottom and the top ground planes are

$$\begin{aligned} H_{y\Sigma}^{bot}(s,y) =& J_{g1}(s,y) = \frac{I_S}{\pi \cdot w_s} \\ & \cdot \int\limits_{s-w_s/2}^{s+w_s/2} \sum_{n=1}^{\infty} \left(\frac{(-1)^{2n-1} \cdot a_n}{a_n^2 + (y-y')^2} + \frac{(-1)^{2n} \cdot b_n}{b_n^2 + (y-y')^2} \right) dy'; \\ H_{y\Sigma}^{top}(s,y) =& J_{g2}(s,y) = \frac{I_S}{\pi \cdot w_s} \\ & \cdot \int\limits_{s-w_s/2}^{s+w_s/2} \sum_{n=1}^{\infty} \left(\frac{(-1)^{2n-1} \cdot c_n}{c_n^2 + (y-y')^2} + \frac{(-1)^{2n} \cdot d_n}{d_n^2 + (y-y')^2} \right) dy'. \end{aligned} \tag{28}$$

It is important that the current balance

$$I_S = I_{g1} + I_{g2} + \Delta I_1 + \Delta I_2 + \Delta I_3 + \Delta I_4 \tag{29}$$

is always fulfilled. The currents on the finite-width ground planes are calculated as

$$\begin{aligned} I_{g1} &= \int\limits_{-w_g/2}^{w_g/2} H_{y\Sigma}^{bot}(s,y)dy; \\ I_{g2} &= \int\limits_{-w_g/2}^{w_g/2} H_{y\Sigma}^{top}(s,y)dy. \end{aligned} \tag{30}$$

The fluxes from the "tail currents" on the ground planes are calculated as

$$\begin{aligned} \Psi_{tail1} &= \frac{\mu_0}{2\pi} \int\limits_{w_g/2}^{\infty} J_{g1}(y) \int\limits_{-\infty}^{-R} \frac{R-z}{(R-z)^2 + y^2} dz dy; \\ \Psi_{tail2} &= \frac{\mu_0}{2\pi} \int\limits_{-\infty}^{-w_g/2} J_{g1}(y) \int\limits_{-\infty}^{-R} \frac{R-z}{(R-z)^2 + y^2} dz dy; \end{aligned}$$

$$\Psi_{tail3} = \frac{\mu_0}{2\pi} \int\limits_{w_g/2}^{\infty} J_{g2}(y) \int\limits_{-\infty}^{-R} \frac{R + h_1 + h_2 - z}{(R + h_1 + h_2 - z)^2 + y^2} dz dy;$$
$$\Psi_{tail4} = \frac{\mu_0}{2\pi} \int\limits_{-\infty}^{-w_g/2} J_{g2}(y) \int\limits_{-\infty}^{-R} \frac{R + h_1 + h_2 - z}{(R + h_1 + h_2 - z)^2 + y^2} dz dy. \quad (31)$$

In (31), $R = d/2$ is the half of the ground plane thickness. When the edge-current distribution on the rounded edges is introduced as $J_{edge\ i} = \Delta I_i/(\pi R)$, $i = 1 \ldots 4$, the magnetic fields associated with the fluxes from the edges are calculated similar to (20) and (21),

$$H^{top}_{y\,edge\,1,2} = \int\limits_0^{\pi/2} \frac{J_{edge\,1,2} R \cdot \left(\frac{w_g}{2} + R\sin\alpha\right)}{2\pi\left(\left(\frac{w_g}{2} + R\sin\alpha\right)^2 + (R\cos\alpha - z)^2\right)} d\alpha;$$
$$H^{bot}_{y\,edge\,1,2} = \int\limits_0^{\pi/2} \frac{J_{edge\,1,2} R \cdot \left(\frac{w_g}{2} + R\sin\alpha\right)}{2\pi\left(\left(\frac{w_g}{2} + R\sin\alpha\right)^2 + (R\cos\alpha + z)^2\right)} d\alpha; \quad (32)$$

and

$$H^{top}_{y\,edge\,3,4} = \int\limits_0^{\pi/2} \frac{J_{edge\,3,4} R \cdot \left(\frac{w_g}{2} + R\sin\alpha\right)}{2\pi\left(\left(\frac{w_g}{2} + R\sin\alpha\right)^2 + (R\cos\alpha - z + h_1 + h_2)^2\right)} d\alpha;$$
$$H^{bot}_{y\,edge\,3,4} = \int\limits_0^{\pi/2} \frac{J_{edge\,3,4} R \cdot \left(\frac{w_g}{2} + R\sin\alpha\right)}{2\pi\left(\left(\frac{w_g}{2} + R\sin\alpha\right)^2 + (R\cos\alpha + z + h_1 + h_2)^2\right)} d\alpha \quad (33)$$

Then the corresponding fluxes are calculated as in (22).

The results of the computations for a stripline geometry with an offset of the signal strip are presented in Figures 5 and 6. Figure 5 shows the mutual inductance as a function of an offset of a signal trace from the center in the horizontal plane s/w_g. The signal trace is equidistant from the ground planes ($h_1 = h_2 = h/2$). There is an increase of the mutual inductance as the trace is shifted to the edge of the stripline. The mutual inductance is higher, when the ground plane width is narrower. However, when the ground plane is wide, the increase in the mutual inductance is more abrupt, when the trace

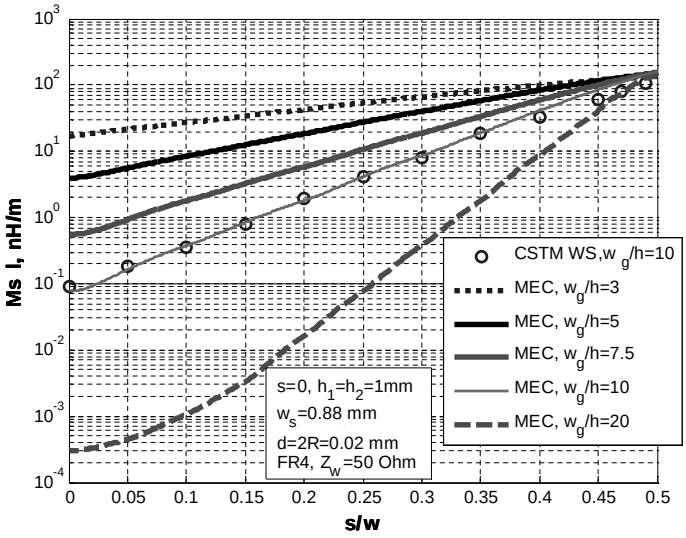

Figure 5. Mutual external inductance in a stripline with an offset of a signal trace from the center in the horizontal plane. The signal trace is equidistant from the ground planes.

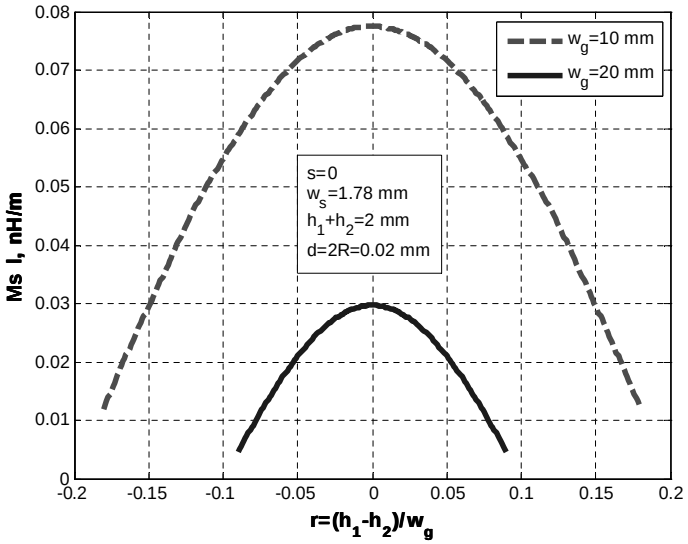

Figure 6. Dependence of the mutual inductance in a stripline upon the vertical offset of the strip. The strip is centered in the horizontal plane — MEC modeling results.

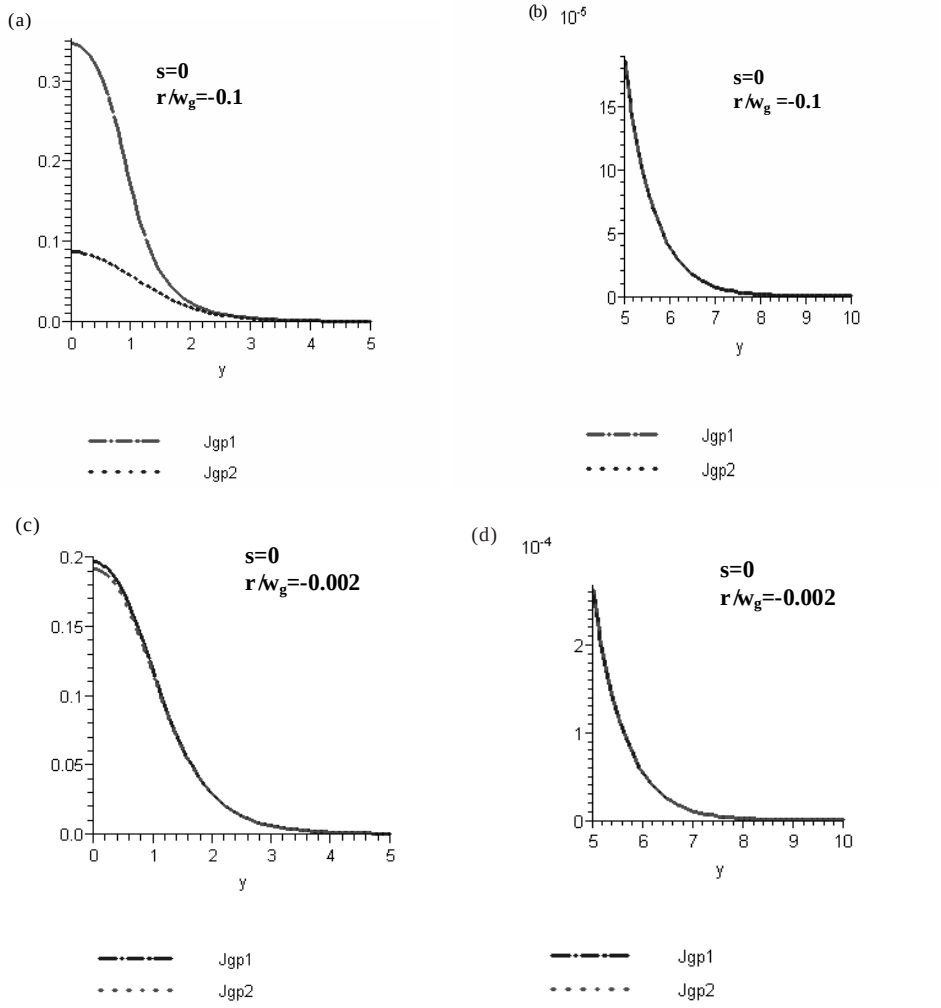

Figure 7. Current density distribution $J_{gp1,2}$ [A/m]: (a) within the ground plane width $(0, w_{gp}/2)$, vertical offset $r/w_g = -0.1$; (b) "tail" ground plane current density $(w_{gp}/2, \infty)$, vertical offset is $r/w_g = -0.002$; (c) within the ground plane width $(0, w_{gp}/2)$, vertical offset is $r/w_g = -0.002$; (d) "tail" ground plane current density $(w_{gp}/2, \infty)$, vertical offset is $r/w_g = -0.002$. Stripline parameters are $w_s = 1.78\,\text{mm}$, $w_g = 10\,\text{mm}$, $h_1 = 1.8\,\text{mm}$, $h_2 = 0.2\,\text{mm}$, $d = 2R = 0.02\,\text{mm}$, and $I_s = 1\,\text{A}$. The horizontal offset parameter $s = 0$.

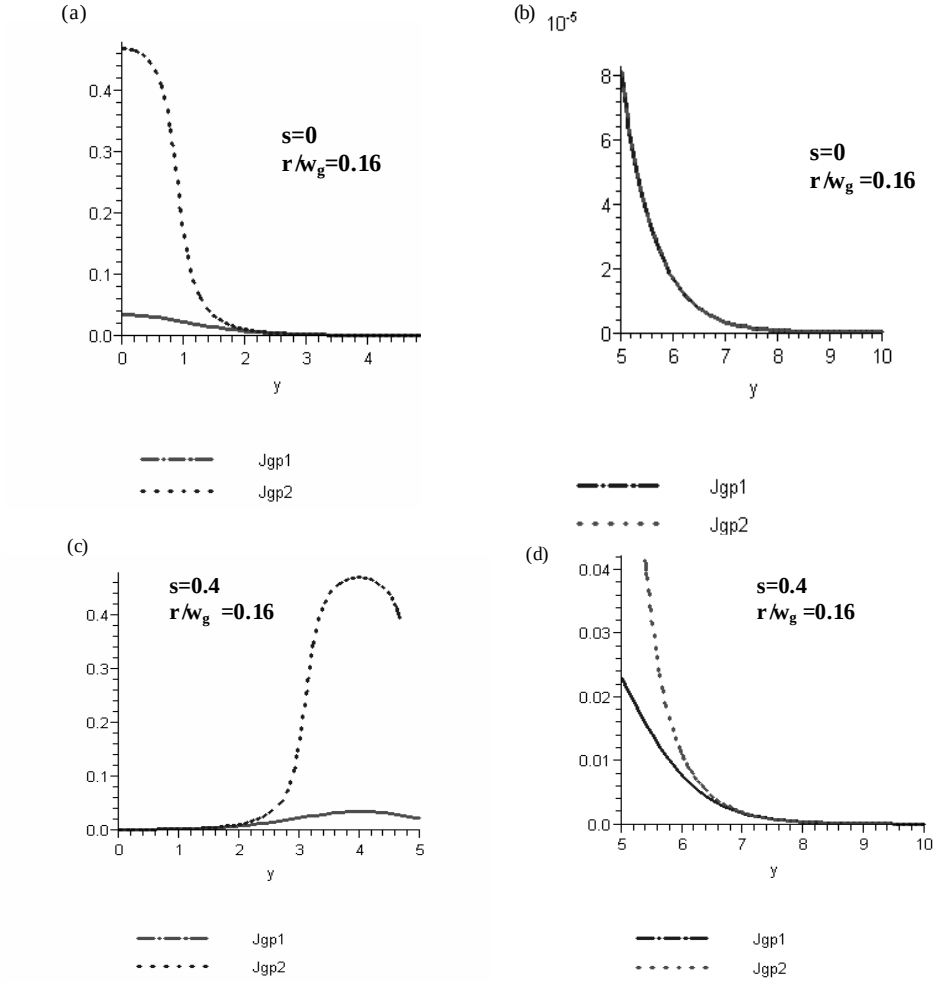

Figure 8. Current density distribution $J_{gp1,2}$ [A/m]: (a) within the ground plane width $(0, w_{gp}/2)$, horizontal offset $s = 0$; (b) "tail" ground plane current density $(w_{gp}/2, \infty)$, horizontal offset $s = 0$; (c) within the ground plane width $(0, w_{gp}/2)$, horizontal offset $s = 0.4$; (d) "tail" ground plane current density $(w_{gp}/2, \infty)$, horizontal offset $s = 0.4$. Stripline parameters are $w_s = 1.78\,\text{mm}$, $w_g = 10\,\text{mm}$, $h_1 = 1.8\,\text{mm}$, $h_2 = 0.2\,\text{mm}$, $d = 2R = 0.02\,\text{mm}$, and $I_s = 1\,\text{A}$. The vertical offset parameter $r = (h_1 - h_2)/w_g = 0.16$.

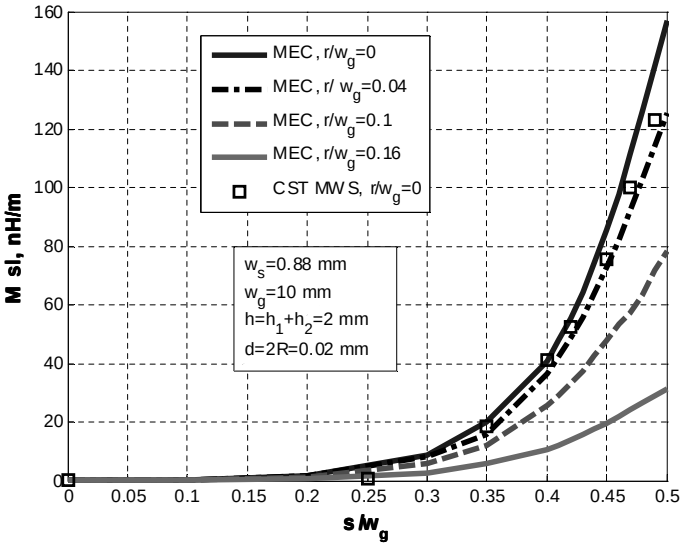

Figure 9. Dependence of the mutual inductance in a stripline upon the horizontal offset of the signal trace for different vertical offsets.

becomes closer to the edge. There is only some decrease of mutual inductance, when the signal trace is shifted in the vertical direction from the center, as is shown in Figure 6. The effect is stronger when the ground planes are narrower. When ground planes are comparatively wide (at least, $w_g/(h_1+h_2) > 1$), there is not much difference whether a signal trace is centered vertically or not. Computations using Maple 10 show that the closer the signal trace to a ground plane, the higher is the magnitude of the current density on this ground plane, as is seen from Figures 7 and 8. However, the "tail" current density outside the region $(-w_g/2, w_g/2)$ is almost independent of the vertical position of the trace, if the trace is centered in horizontal plane ($s = 0$). This is the reason why the vertical offset only does not affect the external mutual inductance.

However, if there is also the horizontal offset of the signal trace, the variation of mutual inductance is substantial. Our computations are consistent with those obtained in [21].

Figure 7 shows the combined effect of both offsets — vertical and horizontal, at the fixed ($w_g = 10\,\text{mm}$) widths of the ground planes. Mutual inductance as a function of relative horizontal offset increases exponentially as $s/w_g \to 0.5$. Some slight increase in mutual inductance due to the vertical offset of the signal trace can be seen.

3. CONCLUSIONS

A *method of edge currents* proposed in [1], is applied herein for calculating the mutual inductance associated with fringing magnetic fields in symmetrical and asymmetrical stripline structures (with the signal trace offset from the center both in the horizontal and vertical directions). This method employs a quasi-static approach, image theory, superposition, and a direct magnetic field integration technique. The residue surface ground-plane currents on the tails that are cut off are redistributed on the edges of the ground planes of finite thickness. At zero ground plane thickness, these edge currents shrink to filamentary. The mutual external inductance is determined mainly by the magnetic fluxes produced by these edge currents. For a stripline geometry, there is a good agreement with full-wave numerical simulations using *CST Microwave Studio*. The presented approach may be also used for the analysis of multiconductor planar transmission lines, since it is based on the superposition principle.

The practically important conclusion is the following. In a stripline geometry, there is no much increase in the external ground plane inductance, until the signal trace is shifted at the position of approximately $s/w_g < 0.4$ from the edge. This means that if the signal trace should not be closer than 10% of the ground plane width. These values are the general and approximate recommendations for a designer. However, mutual ground plane inductance should be evaluated for every particular case, since it depends on the offset of the signal trace from the center (both horizontal and vertical in the stripline geometry), on the width of the ground plane, height of the transmission line, width of the trace, and the thickness of the ground planes. The presented *Method of Edge Currents* gives the upper limit of the possible mutual inductance associated with fringing magnetic fields, so, for a benefit of a designer, practical edge values of mutual inductance should be below values calculated using the presented method.

ACKNOWLEDGMENT

CST MICROWAVE STUDIO$^{(R)}$ was used in the preparation of this paper under a collaboration agreement between UMR and CST of America, Inc.

REFERENCES

1. Koledintseva, M. Y., J. L. Drewniak, T. P. van Doren, D. J. Pommerenke, M. Cocchini, and D. M. Hockanson, "Method of edge currents for calculating mutual external inductance in a microstrip structure," *Progress In Electromagnetic Research*, accepted for publication, 2008.
2. Hubing, T. H., T. P. van Doren, and J. L. Drewniak, "Identifying and quantifying printed circuit board inductance," *Proc. 1994 IEEE Int. Symp. Electromagnetic Compatibility*, 205–208, Chicago, IL, USA, Aug. 1994.
3. Hockanson, D. M., J. L. Drewniak, T. H. Hubing, T. P. van Doren, F. Sha, and C. W. Lam, "Quantifying EMI resulting from finite-impedance reference planes," *IEEE Trans. Electromagn. Compat.*, Vol. 39, No. 4, 286–297, Nov. 1997.
4. Ooi, T. H., S. Y. Tan, and H. Li, "Study of radiated emissions from PCB with narrow ground plane," *Int. Symp. Electromagnetic Compatibility*, No. 20A101, 552–555, Tokyo, May 17–21, 1999.
5. Hockanson, D. M., J. L. Drewniak, T. H. Hubing, T. P. van Doren, F. Sha, and M. Wilhelm, "Investigation of fundamental EMI source mechanisms driving common-mode radiation from printed circuit boards with attached cables," *IEEE Trans. Electromagn. Compat.*, Vol. 38, No. 4, 557–565, Nov. 1996.
6. Xiao, F. and Y. Kami, "Common- and differential-mode components at asymmetric pattern-layout lines on PCB," *Proc. PIERS 2006*, Tokyo, Japan, Aug. 2–5, 2006.
7. Nikellis, K., N. K. Uzunoglu, Y. Koutsoyannopoulos, and S. Bantas, "Full-wave modeling of stripline structures in multilayer dielectrics," *Progress In Electromagnetics Research*, PIER 57, 253–264, 2006.
8. Ikami, S. and A. Sakurai, "Analysis of 20H rule applied to printed circuit board," *Proc. PIERS 2006*, 1P3, Tokyo, Japan, Aug. 2–5, 2006.
9. Arshadi, A. and A. Cheldavi, "Simple and novel model for edged microstrip line (EMTL)," *Progress In Electromagnetics Research*, PIER 65, 247–259, 2006.
10. Nashemi-Nasab and A. Cheldavi, "Coupling model of the two orthogonal microstrip lines in two-layer PCB board (Quasi-TEM approach)," *Progress In Electromagnetics Research*, PIER 60, 153–163, 2006.

11. Kuo, L.-C., H.-R. Chuang, Y.-C. Kan, T.-C. Huang, and C.-H. Ko, "A study of planar printed dipole antennas for wireless communication applications," *Journal of Electromagnetic Waves and Applications*, Vol. 21, No. 5, 637–652, 2007.
12. Ren, W., J.Y. Deng, and K. S. Chen, "Compact PCB monopole antenna for UWB applications," *Journal of Electromagnetic Waves and Applications*, Vol. 21, No. 10, 1411–1420, 2007.
13. Eldek, A. A., "Numerical analysis of a small ultrawideband microstrip-fed tab monopole antenna," *Progress In Electromagnetics Research*, PIER 65, 59–69, 2006.
14. Ali, M. and S. Sanyal, "A numerical investigation of finite ground planes and reflector effects on monopole antenna factor using FDTD technique," *Journal of Electromagnetic Waves and Applications*, Vol. 21, No. 10, 1379–1392, 2007.
15. Nikellis, K., N. K. Uzunoglu, Y. Koutsoyannopoulos, and S. Bantas, "Full-wave modeling of stripline structures in multilayer dielectrics," *Progress In Electromagnetics Research*, PIER 57, 253–264, 2006.
16. El Sabbagh, M. A., H.-T. Hus, K. A. Zaki, P. Pramanick, and T. Dolan, "Stripline transition to ridge waveguide bandpass filters," *Progress In Electromagnetics Research*, PIER 40, 29–53, 2003.
17. Bankov, S. and J. An, "Design and experimental investigation of stripline antennas," *Journal of Communications Technology and Electronics*, Vol. 52, No. 8, 865–875, 2007.
18. Xiao, F. and Y. Kami, "Modeling and analysis of crosstalk between differential lines in high-speed interconnects," *Proc. PIERS 2007*, 488–492, Prague, Czech Republic, Aug. 27–30, 2007.
19. Yang, Y., G. Wang, and J. Xue, "A quick parasitic extraction tool for IC interconnections," *Proc. PIERS 2006*, Tokyo, Japan, Aug. 2–5, 2006.
20. Qin, Y., A. Fang, J. Hu, W. Zhou, and M. Zhang, "Modified equivalent circuit model of microwave filter with LTCC technique," *PIERS Online*, Vol. 2, No. 3, 292–296, 2006.
21. Holloway, C. L. and E. F. Kuester, "Closed-form expressions for the current densities on the ground planes of symmetric stripline structures," *IEEE Trans. on Electromagn. Compat.*, Vol. 49, No. 1, 49–57, Feb. 2007.
22. Semenov, N. A., *Technical Electrodynamics*, Section 10.6, 251–254, Svyaz, Moscow, Russia, 1973 (in Russian).